Int. J. Metrol. Qual. Eng. **8**, 20 (2017)

DOI: 10.1051/ijmqe/2017011

International Journal of Metrology and Quality Engineering

Available online at:
www.metrology-journal.org

RESEARCH ARTICLE OPEN ACCESS

Development of ^{137}Cs irradiation facility for metrological application

Mohamed A. Hassan, Enas Esmat, and Ahmed R. El-Sersy*

Department of Ionizing Radiation Metrology, National Institute for Standards (NIS), El-Haram, Giza, Egypt

Received: 10 November 2016 / Accepted: 2 May 2017

Abstract. In this work, ^{137}Cs irradiation facility at the National Institute of Standards (NIS) was developed to enhance the calibration processes. Different thickness lead sheets were used for beam attenuation, to enlarge the ^{137}Cs dose range. Ambient dose equivalent rate, $H^*(10)$ was measured using two ionization chambers at a different source-detector distances (SDDs) and a lead sheet thickness. The deviation from the inverse square law for the dose–SDD relationship was obtained. The beam flatness of unattenuated and the lead attenuated beam was measured. The attenuation coefficient for the used lead sheets was obtained and correlated to the broad beam geometry. The room scattering was studied in detail. The uncertainty of the measured doses was calculated. It was found that the inverse square law is verified well at SDD $\geq$ 2 m. The measured attenuation coefficient for lead attenuators is affected by the broad beam geometry. The contribution of the scattering component of the dose at a certain SDD is the major source of uncertainty since it extracted a value of 1.05%, while the combined uncertainty from all other factors affecting the dose measurements is 1.34%.

Keywords: ionizing radiation / radiation protection / Cs-137 / scattering / irradiation facility

1 Introduction

The Ionizing Radiation Metrology Lab (IRML), in the Egyptian National Institute of Standard (NIS), is one of the Secondary Standard Dosimetry Lab (SSDL) of the IAEA and WHO network. The major SSDLs activities used to provide traceability to customers. One of such activities is the calibration of radiation dosimeters in terms of ambient dose equivalent rate $H^*(10)$ (mSv/h) [1–5].

According to the recent international protocols, ^{137}Cs is used as a good beam quality for calibration in the range of radiation protection [6–10]. ^{137}Cs reference beam at NIS is characterized to be used in survey meter calibrations and other radiation detectors at protection level as well. ^{137}Cs high dose rate enforces the need of lead attenuators in order to cover the range of protection level calibrations [1]. Moreover, irradiation facilities should be characterized for use in calibration purposes and intercomparison with standard laboratories [2,11].

The main objective of this article is to perform some developments of ^{137}Cs irradiation facility to improve the accuracy of the calibration process and facilitate the calibration procedure for the radiation detectors by studying the beam divergence in the irradiation room, scattering component and evaluate the uncertainty budget for standard doses.

2 NIS ^{137}Cs irradiation facility

^{137}Cs irradiator, used in this work, is model GB150 manufactured by Atomic Energy of Canada Ltd in 1970 with an original activity of 37×10^{12} Bq. A lead cone with angle of 15° was used for beam collimation. The scattering contribution after adding this collimator was reduced by about 12% at a distance of 2 m from the source [1].

A set of three lead sheet attenuators with a surface area of 26 cm × 32 cm and different thicknesses of 2.1, 3 and 4.1 cm, respectively, were used separately or in a combined manner to provide a beam intensity reduction more than 1000 times of its original value. The lead absorbers were placed at the exit of the collimation cone of the irradiator (see Fig. 1).

In the front of the irradiation system, there is a stand fixed on a platform. The stand was designed to be moved in x, y and z directions. It is used for supporting the calibrated devices in the center of the radiation field with the aid of a laser system. The source-detector distance (SDD) was determined by a measuring rod fixed on the platform. The stand management functions are carried out by a portable control panel for x and y-direction and manually controlled for z direction. A video surveillance system is used for remote the reading of indications on the scales of the calibrated devices. Recently the stand position can be controlled from outside the irradiation room for different SDD. This was carried out by fixing a small video camera

* Corresponding author: aelsersy@yahoo.com

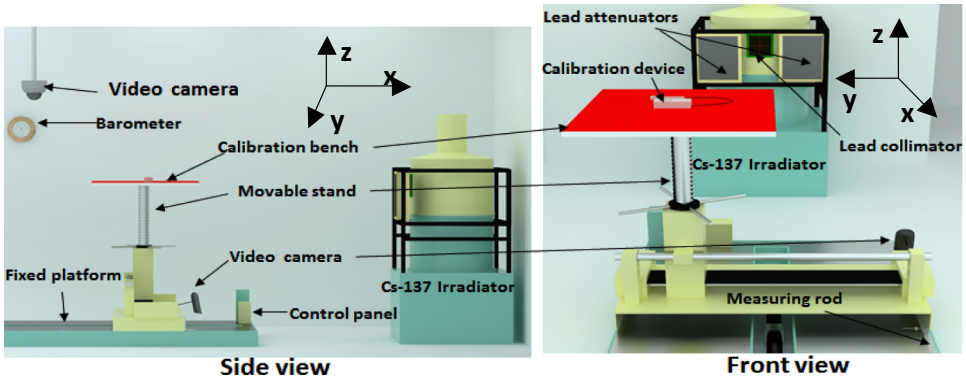

Fig. 1. Front and side view of NIS ^{137}Cs irradiation facility.

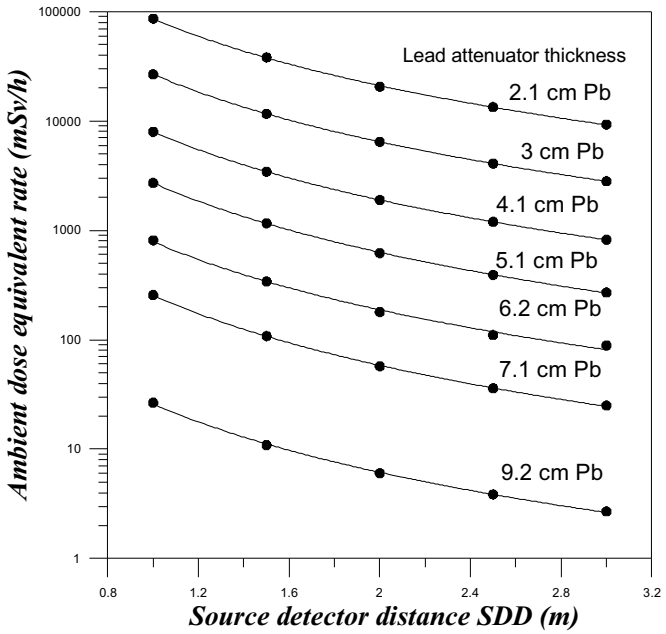

Fig. 2. The ambient dose equivalent rate $H^*(10)$ for NIS ^{137}Cs source at different SDD using the lead sheets attenuators and their combinations.

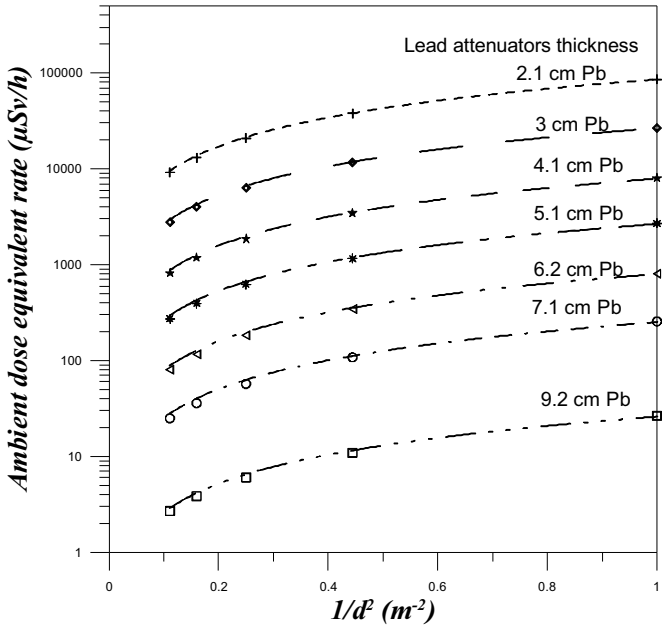

Fig. 3. Verification of the inverse square law for a lead attenuated beam of ^{137}Cs source.

and indicator with the stand normal to the measuring rod. Figure 1 shows ^{137}Cs irradiation facility, which includes a cylindrical shield with a rectangular window for exposure. Holders of steel were designed and constructed to hold lead sheets used for attenuation in front of the exposure window.

3 Ambient dose equivalent rate measurements

Ambient dose equivalent rate $H^*(10)$ for the^{137}Cs source was measured using NIS secondary standard dosimeter system which was composed of UNIDOS electrometer and two ion chambers (NE2530 and M-32002 PTW). The NE 2530 chamber has a volume of 30 cm^3. It was calibrated at the BIPM in 2012 in terms of $H^*(10)$. The M-32002 PTW chamber has a volume of 1000 cm^3, which was used for determining dose rate less than 1 mSv/h.

Figure 2 shows the ^{137}Cs output doses as a function of SDD for different lead sheet attenuators. From this figure, one can notice that using the lead sheet attenuators can cover a wide range of doses, which is suitable for all calibrations of different scales of survey meters and pocket dose meters.

The unmeasured doses at any other distances can be calculated by inverse square law. To determine the deviation of calculating doses from the measured ones, the values of output doses were plotted with $1/d^2$ and represented in Figure 3. From this figure, it is obvious that the accuracy of the linear fitting is very high (see Tab. 1) that reflects the using of the inverse square law to get an unmeasured dose at any arbitrary distance within reasonable uncertainty, especially for primary beam. However, the difference between the calculated values by the inverse square law fitting to the measured one is significant for the attenuated beam at SDD 1 and 1.5 m, which is equal to 8.2% and 5%, respectively. This may be attributed to the

Table 1. The coefficient of determination, R^2 of the linear fitting curves of $H^*(10)$ rate with $1/d^2$.

Lead attenuator thickness	R^2 using M-32002 PTW chamber	R^2 using NE 2530 chamber
No attenuators	0.9999	0.9999
2.1 cm	0.9999	0.9999
3 cm	0.9997	0.9999
4.1 cm	0.9996	0.9997
5.1 cm	0.9995	0.9993
6.2 cm	0.9992	0.9986
7.1 cm	0.9988	0.9973
9.2 cm	0.9987	0.9888

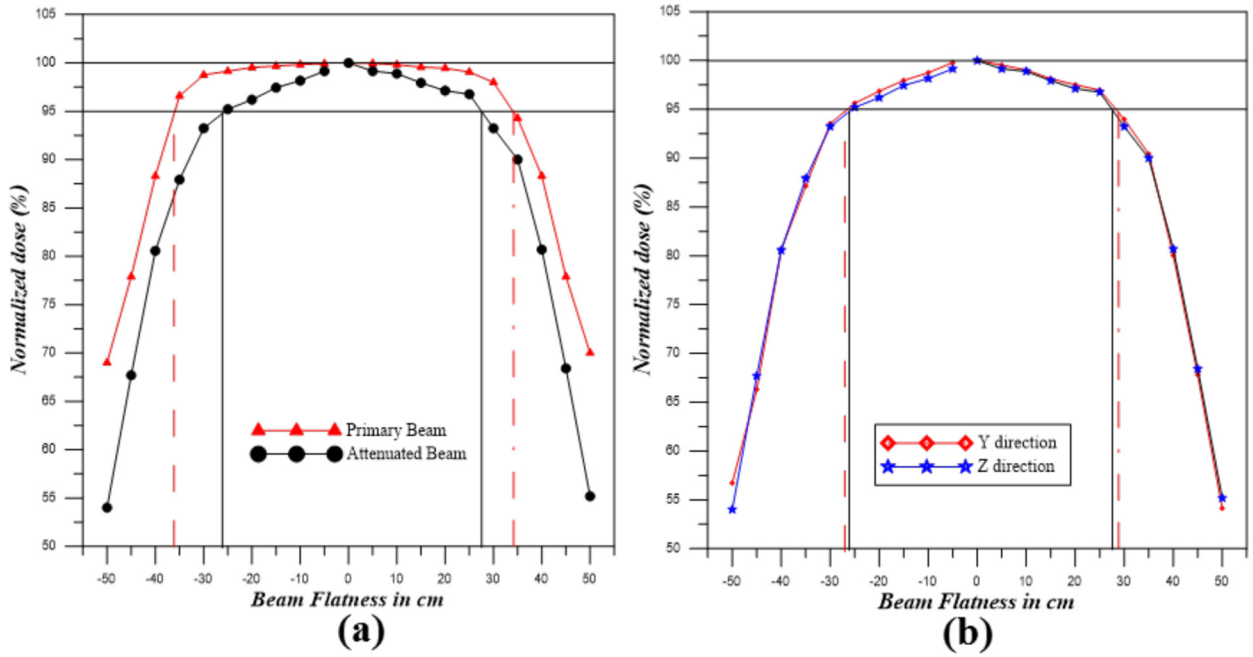

Fig. 4. Typical useful beam dimension at 3 m SDD (a) primary and attenuated beam; (b) Y and Z direction for attenuated beam.

position of the chambers near the attenuator since this difference does not exceed 0.17% at 1 m for the primary beam condition.

Many investigators using some models for fitting the calculated dose with distance [2] for the primary beam only not for the attenuated beam [2]. Therefore, the contribution of the scattered radiations from the attenuator affects the measurements near the source as the obtained data.

A comparison between the coefficient of determination (R^2) for the linear fitting curves of $H^*(10)$ with $1/d^2$ is tabulated in Table 1 for the two chambers used. The obtained dose values represented that there is an agreement between doses obtained by the two chambers in high dose range while in the low dose range, the 1000 cm^3 (M-32002 PTW) chamber gives more accuracy in the $H^*(10)$ rate.

4 Beam flatness measurements

Assuming the SDD is the x axis and y, z are the lateral and vertical axes, respectively (see Fig. 1), the beam flatness was measured in y and z-direction to deduce the beam flatness measurements. Using NE 2530 chamber, for both primary and 2.1 mm lead sheets attenuated beams at an SDD value of 3 m. Figure 4a and b represents a comparison between the beam flatness at Y axis of primary and attenuated beams (Fig. 4a) and the attenuated beam for both Y and Z axes (Fig. 4b), respectively. From the data of Figure 4, it is obvious that the divergence of the primary beam, is larger than the attenuated one (Fig. 4a). However, the field size is the same in Y and Z direction (Fig. 4b). Moreover, the field size at 3 m SDD for the direct and

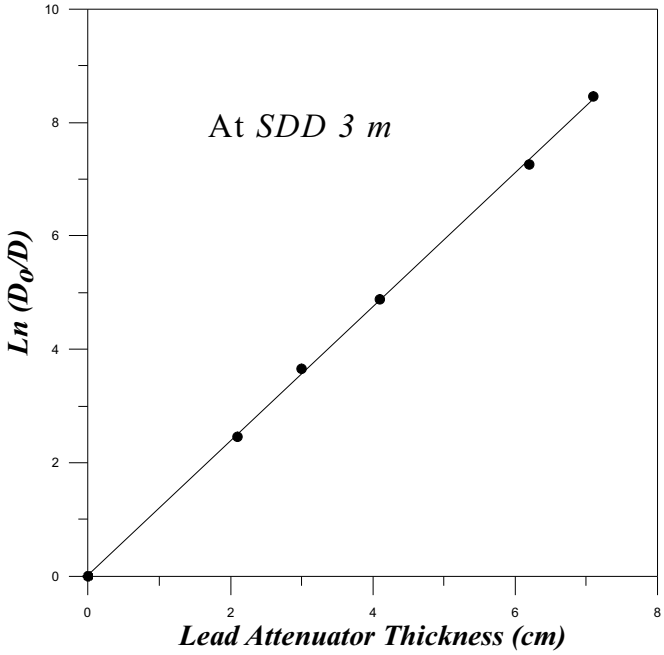

Fig. 5. The Ln (D_o/D) as a function of lead thickness at SDD 3 m using NE 2530 chamber.

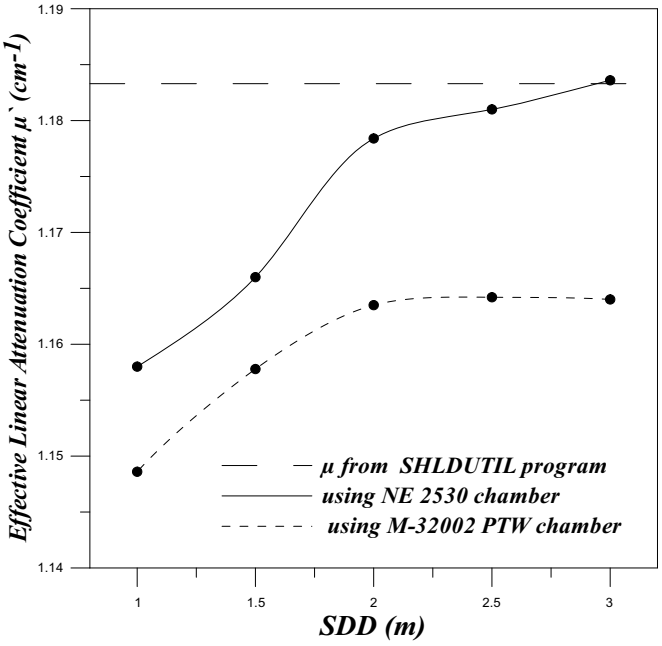

Fig. 6. A comparison between the measured effective linear attenuation coefficient $\mu\prime$ and using NE 2530 and M-32002 PTW to the theoretically calculated μ.

attenuated beams is about 70 and 55 cm, respectively, which reflected a reduction of the field size by about 21% of its original value due to the beam attenuation.

5 Performance of the lead sheets

To check the performance of the lead sheets used as an attenuator, the effective linear attenuation coefficient $(\mu\prime)$ was determined by plotting the chamber reading with the lead sheet thickness.

Figure 5 shows Ln (D_o/D) as a function of lead thickness at SDD 3 m using NE 2530 chamber (where D_o and D is the chamber reading without and with the lead sheets attenuators, respectively). The effective linear attenuation coefficient $\mu\prime$ was obtained from the slope of the linear fitting of the curve in Figure 5 which is nearly equal to the linear attenuation coefficient μ $(1.1833\,\mathrm{cm}^{-1})$ that calculated by the SHLDUTIL program [12] (based on the table of lead linear attenuation coefficient vs. energy without significant uncertainty value [13]). The agreement between values of $\mu\prime$ and μ could be attributed to the performance of the lead sheet used as an attenuator and the position of the chamber away from the lead sheet attenuators. Moreover, the measurements were repeated to obtain effective linear attenuation coefficient $\mu\prime$ at different SDD. The coefficient of determination, R^2 for the linear fitting of Figure 5 and the others repeated measurements were 0.999 that extract uncertainty of 0.1%.

Figure 6 shows a comparison between the measured effective linear attenuation coefficient $\mu\prime$ using NE 2530 chamber and M-32002 PTW chamber with different SDD. The two curves represent the significant variation between $\mu\prime$ and μ with the decrement of SDD. The variation between $\mu\prime$ and μ is normally occurring in broad beam geometry [14]. One of the solutions to this problem is to increase the SDD to reduce the effect of the secondary beam scattering that produced in the lead attenuator. Certainly, in the broad beam condition, the ratio between the distances of the detector from the attenuator to beam width should be large enough to perform the setup as that of narrow-beam geometry. Therefore, it is recommended to perform the calibration at SDD ≥ 2 m.

Moreover, the variation of the attenuation coefficient measured by the two chambers used may be related to the geometry and the effective volume of each one and their scattering contribution.

6 Scattering radiation measurements

The scattering radiation was evaluated by the shadow-shield method. In this method, a lead cone is located between the source and the chamber to avoid the primary photons to reach the chamber. The chamber is completely shielded from the primary radiation and only the scattering radiation reaches of the chamber [15,16]. The lead cone thickness that used in this work can reduce the primary radiation intensity in the detector position less than 0.4% of its original value. The NE-2530 chamber was used for those measurements at different SDD. The scattering radiation dose was measured when the shadow lead cone was positioned in between the chamber and the source at a certain distance. The ratio of the scattering radiation dose to the total one was calculated for different distances.

Figure 7 shows the relation between the percentage value of the room, scattering and SDD for both primary and attenuated beam. It is remarkable that the scattering percentage increased with SDD up to 1.2 m and has no significant difference between the primary and attenuated

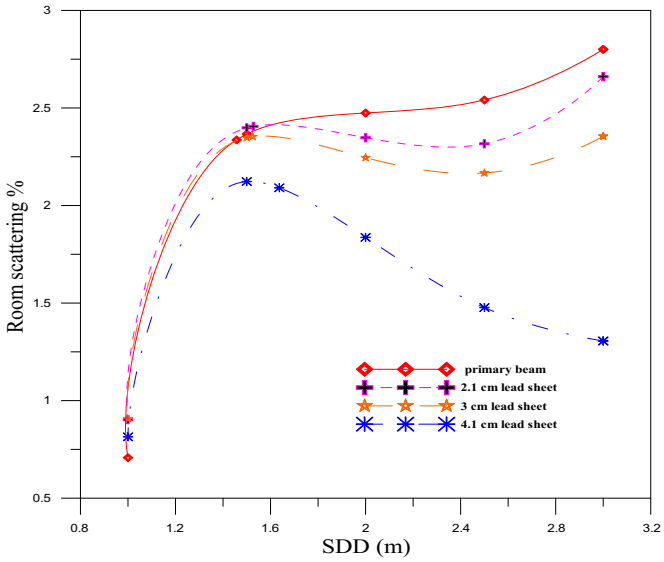

Fig. 7. The room scattering (%) as a function of SDD by beam shadow method.

beams at SDD 1 m. However, the SDD increases the scattering percentage decreases for the attenuated beam than the primary one. Moreover, as the attenuator thickness increased the scattering decreased, which was very significant at SDD 3 m. These results are in agreement with the beam flatness measurements, which have shown before, the effect of the attenuators on the reduction of the field size. The addition of 4.1 cm lead attenuator reduced the room, scattering percentage less than half of its primary beam value at SDD 3 m.

7 Uncertainty calculations

The model that used to calculate the uncertainty in the measurements is based on the combination of the uncertainties in each parameter in the equation used in ambient dose equivalent rate calculation $H^*(10)$ [6,7]

$$H^*(10) = MN_k \prod_i K_i, \tag{1}$$

where M (nC) is the reading of the electrometer, N_k (mSv/nC) is the chamber calibration factor which obtained from the calibration certificate and K_i are set of dimensionless correction factors to include:

- k_{tp} is a factor to correct for a departure of air density from reference conditions due to the variation of temperature and pressure;
- k_{dist} is a factor to correct for deviation of chamber position (distance from the source);
- k_{sct} is the factor to correct the contribution of the secondary photon scattering due to beam surrounding geometry;
- k_{other} is a factor including all the corrections whose uncertainties are too small to consider individually in the uncertainty budget as an electrometer calibration factor, saturation due to ion recombination, polarity effect, and leakage current.

The uncertainty due to independent parameters in equation (1) may have a statistical component (type A) or regular ones (type B) and the total combined uncertainty was calculated from equation (2) [17].

$$U_C = \sqrt{\sum U_A^2 + \sum U_B^2}. \tag{2}$$

Each source of uncertainty is considered individually as follows:

- statistical uncertainty due to repeatability and reproducibility of dose measurements were 10 readings were taken and the standard deviation was used for repeatability determination (type A);
- the uncertainty of the dosimetry system (ionization chamber and electrometer) which are contained uncertainty of a dosimeter calibration factor, dosimeter stability, reading resolution. All these components have type B by considering rectangular distribution where their values are 0.54%. The leakage of the measured charge and saturation due to ion recombination has type A combined uncertainty value of 0.17%.
- uncertainty due to a position of ion chamber which contains uncertainty due to the radial uniformity of chamber position and other due to SDD measurements which calculated from the inverse square law. This component of uncertainty has a value of 0.2% type B from the calibration certificate of meter used in distance measurements and a value of 0.2% type A due to the repeatability of longitudinal and lateral dose measurements;
- uncertainty due to the measurements of environmental conditions (temperature and pressure, K_{TP}) which has a value of 0.18% type B component from calibration certificate of barometer and thermometer and a value of 0.35% type A from repeatability of an impact of ambient on dose measurements;
- uncertainty due to beam scattering: the uncertainty in the measurements of beam scattering depends on the summation of uncertainties in the primary beam measurements and summation of the uncertainties of the secondary beam measurements which are considered as type B. While, the type A uncertainty is the standard uncertainty due to the repeatability in the beam scattering measurements.

The numerical values of the uncertainties of the measured $H^*(10)$ were estimated considering different effective components and were tabulated in the budget of Table 2.

The expanded standard uncertainty of output $H^*(10)$ of ^{137}Cs source is 2.68% with a coverage factor of 2 and confidence level 95%.

8 General discussion

This work is very important for the characterization of NIS irradiation facilities used for metrological applications. The procedure is emphasized that it is important to verify the inverse square law for the beam used in calibration. In the case of using lead sheet attenuators, the

Table 2. Uncertainty budget for the measurements.

Source of uncertainty	Type A value (%)	Type B value (%)
1. Statistical uncertainty		
Repeatability of measurements	0.06	–
Reproducibility of measurements	0.35	–
2. Uncertainty of dosimeter reading that include: calibration factor, resolution of reading, stability and ion recombination	0.17	0.52
3. Uncertainty due to position of ion chamber (uniformity and distance)	0.2	0.2
4. Uncertainty due to the measurements of environmental conditions, K_{TP} (temperature and pressure)	0.35	0.18
5. Uncertainty due to beam scattering	0.35	1

Combined relative standard uncertainty = 1.34%.

beam flatness studies are necessary to perform (see Fig. 4) especially for the calibration that needs a large field size as the exposure of TLD cards using slab phantom. However, the reduction of beam width after adding the lead attenuators reflects the variation of beam divergence. Moreover, the scattering component is affected by the attenuator thickness at different SDD (see Fig. 7) that should be considered in the uncertainty calculations. Since, the contribution of the scattering component of the dose at a certain SDD is the major source of uncertainty in the measurements. The calculation of uncertainty in dose measurements in this work extracted a value of 1.05% due to beam scattering while the combined uncertainty from all other factors affecting the dose measurements is 1.34%. So it is recommended to calculate the scattering values using the suggested procedure taking into consideration the dimension of the irradiation room and the source activity used.

9 Conclusion

The new development in the NIS calibration facility for the protection level improves the accuracy in the calibration process. The addition of lead attenuators reduces the beam flatness by 21% till the useful beam dose level 95%. The ambient dose rate measurements show that the ^{137}Cs source with the lead attenuators can cover all scales of radiation measuring instrument needed to be calibrated at NIS. The effect of the attenuation on the reduction of the room scattering was significant at SSD 3 m. The verifications of the inverse square law and beam exponential attenuation evaluate that the calibration has to perform at SDD $\geq$ 2 m.

The authors express their deep thanks and great appreciation to Prof. Dr. M.M. Mansy for his help in the ^{137}Cs irradiation facility, development of IRML, and for his grateful discussion and continuous advice.

References

1. A.R. El-Sersy, N.E. Khaled, S.A. Eman, Characterization of Cs-137 beam for calibration and dosimetric applications, Int. J. Nucl. Energy Sci. Eng. **2**, 62–64 (2012)
2. R. Minniti, S.M. Seltzer, Calibration of a 137Cs γ-ray beam irradiator using large size chambers, Appl. Radiat. Isot. **65**, 401–406 (2007)
3. ISO-4037-1:1996(E), *X and Gamma Reference Radiation for Calibrating Dosimeters and Dose Rate Meters for Determining Their Response as a Function of Photon Energy* (ISO, Geneva, 1996)
4. E. Fernandes, D. Freire, A.C. de Freitas, C.E. de Almeida, The radiation field characteristics of a ^{137}Cs source used for calibration of radiation protection instruments, Appl. Radiat. Isot. **61**, 1425–1430 (2004)
5. R. Nathuram, Photon attenuation characteristics of radiation shielding materials, in *IRPA10* (2005) P-6a-327
6. ISO, *Guide to the Expression of Uncertainty in Measurement*, 2nd edn. (ISO, Geneva, 1995)
7. Safety Reports Series No. 16, *Calibration of Radiation Protection Monitoring Instruments* (International Atomic Energy Agency, Vienna, 2000)
8. CCRI (I)/13-22, International Atomic Energy Agency. Activities of the dosimetry and medical radiation physics section. Activities in 2011 and 2012
9. S.K. Kang, D.J. Rhee, Y.R. Kang, J.K. Kim, D.H. Jeong, Determination of TRS-398 quality factors for Cs-137 gamma rays in reference dosimetry, Prog. Med. Phys. **25**, 123–127 (2014)
10. Y.M. Moon, D.J. Rhee, J.K. Kim, Y.-R. Kang, M.W. Lee, H. Lim, D.H. Jeong, Reference dosimetry and calibration of glass dosimeters for Cs-137 gamma-rays, Prog. Med. Phys. **24**, 140–144 (2013)
11. R. Minniti, L. Czap, Comparison of the air kerma standards for Cs-137 and Co-60 gamma-ray beams between the IAEA and the NIST, Metrologia **48**, 1–8 (2011)
12. J.K. Shultis, R.E. Faw, *SHLDUTIL: A Code for Useful Shielding Data* (Department of Mechanical and Nuclear Engineering, Kansas State University, Manhattan, KS, 2002)
13. J.K. Shultis, R.E. Faw, *Radiation Shielding* (American Nuclear Society, La Grange Park, IL, 2000), ISBN 0-89448-456-7
14. F.H. Attix, *Introduction to Radiological Physics and Radiation Dosimetry* (Wiley VCH, 1986)
15. F. Verhaegan, E. van Dijk, H. Thierens, A. Aalbers, J. Seuntjens, Calibration of low activity Ir-192 brachytherapy sources in terms of reference air kerma rate with large spherical ionization chambers, Phys. Med. Biol. **37**, 2071–2082 (1992)

16. D.R. Steele, C.M. Petrie, K. Herminghuysen, T.E. Blue, Evaluation of the shadow shield technique for the measurement of scattered radiation, Health Phys. **101**, 59–66 (2011)
17. TECDOC-1585, *Measurement Uncertainty: A Practical Guide for Secondary Standards Dosimetry Laboratories* (International Atomic Energy Authority (IAEA), 2008).

Cite this article as: Mohamed A. Hassan, Enas Esmat, Ahmed R. El-Sersy, Development of ^{137}Cs irradiation facility for metrological application, Int. J. Metrol. Qual. Eng. **8**, 20 (2017)